CHEMICAL ENGINEERING TRANSACTIONS
VOL. 52, 2016
A publication of AIDIC
The Italian Association of Chemical Engineering
Online at www.aidic.it/cet
Guest Editors: Petar Sabev Varbanov, Peng-Yen Liew, Jun-Yow Yong, Jiří Jaromír Klemeš, Hon Loong Lam

ISBN 978-88-95608-42-6; **ISSN** 2283-9216
DOI: 10.3303/CET1652159

On the Dependence of Flow Properties on Porosity in an Open-Cell Foam

Ivan I. Mitrichev*, Andrey V. Jhensa, Eleonora M. Koltsova

D. Mendeleev University of Chemical Technology of Russia, 9, Miusskaya sq., Moscow, Russia, 125047
imitrichev@muctr.ru

In this work the flow properties in an open-cell foam are studied at several values of porosity by means of Computational Fluid Dynamics (CFD). Reynold-Averaged Navier Stokes equations are solved (RANS approach) on a finite-volume three-dimensional mesh. The geometry used is a body centered cubic (bcc) or a face centered cubic (fcc) regular packing of spheres, where spheres represent the foam voidage. Analytical expressions for the model porosity are derived. The simulations are performed with the use of k-ε realizable model. The quantitative assessment of pressure drop, flow unifomity and turbulent intensity is given at different levels of porosity. The lowest porosity corresponds to the highest turbulence intensity and pressure drop but the lowest flow uniformity. The highest turbulence intensity is obtained for the fcc geometry. The results confirm that there would be a compomise between the allowed pressure loss and turbulence intensity. This fact should be taken into account when applying open-cell foams for the intensification of mass-transfer limited processes.

1. Intoduction

Open-cell foams are a well-known class of materials that is widely used in a chemical equipment. Ceramic foams are used as thermal insulators, porous particulate filters and, also, as a support for catalysts (Palma et al., 2015). Metal foams are used as automotive catalysts and as heat exchangers because they possess high thermal conductivity. The high porosity, relatively high mechanic strength (Pozzobom et al., 2015) and light weight are other distinctive features of open-cell foams.

Foam has large surface to volume ratio, and due to this fact, it is considered as a potential substitution of monolith honeycomb catalytic carriers. It has already been shown that the foam catalyst and the honeycomb monolith exhibit similar performance in auto-thermal reforming of liquid and gaseous (Palma V. et al., 2012), and in diesel exhaust oxidation (Bach and Dimopoulos Eggenschwiler, 2011). Despite the larger pressure drop, the crucial feature of foam catalyst is an enhanced mass transfer that allows more compact reactors operating under severe mass transfer limitations (Lucci et al., 2016). The mass transfer of reactants to the catalytic wall is affected by the flow pattern in the reactor. For a foam, the uneven structure facilitates the mixing. The additional mixing, also known as turbulent diffusion, is assumed to be performed by the turbulent eddies. This is the reason why the study of flow properties (in particular, the pressure drop, the turbulence level and the flow uniformity) is important for catalytic applications.

Krishnan et al. (2006, 2008), Kumar and Topin (2014) and Dukhan and Suleiman (2014) evaluated the pressure drop using the direct solution of steady-state Navier-Stokes equations. They did not include turbulence model into the calculations. Their computational studies cannot be called the Direct Numerical Simulation (DNS) of turbulent flow, since DNS should be performed as unsteady simulation on a mesh with heavy refinement. The ability to resolve the smallest eddies on the mesh had not been checked in the cited papers. One may call this approach the solution of laminar Navier-Stokes equations (Della Torre et al., 2014).

Both DNS, Reynold-Averaged Navier-Stokes (RANS) simulation and the solution of laminar Navier-Stokes were performed by Della Torre et al. (2014), but they also did not quantify the turbulence intensity and mainly considered the pressure drop prediction.

Please cite this article as: Mitrichev I. I., Jhensa A. V., Koltsova E. M., 2016, On the dependence of flow properties on porosity in an open-cell foam, Chemical Engineering Transactions, 52, 949-954 DOI:10.3303/CET1652159

Several studies that addressed the turbulence quantification (by means of the calculation of time-averaged turbulence characteristics) are a LES simulation by Hutter et al. (2011) and our previous work (Mitrichev et al., 2012). Unfortunately, these studies did not not consider different values of foam porosity.
The purpose of that work is to determine the pressure drop and the turbulence intensity and assess flow uniformity using the idealized foam geometry that consists of spheres. It should be noted, that the state-of-the-art technologies (laser beam techniques, or 3D printing) allow the producton of highly structured foams, so the model used could also serve as their exact representation.

2. The model

2.1 Geometry

The geometry of foam is constructed from spheres. Each sphere serve as a model of the internal surface of a foam cell. Spheres intersect with each other forming circular holes, and these holes correspond to the foam pores. All spheres are packed with intersections into a volume that represents the part of a foam. The total volume of intersecting spheres is a void volume. The ratio of void volume to the total volume of the part of the foam studied is a porosity. The microporosity of struts is not considered as subtly affecting the macroscopic flow structure. So, one should hereafter understand a macroporosity under the term “porosity”.
There are two dense packings of spheres that are well-known from crystallography: the body centered cubic (bcc) and the face centered cubic (fcc) packings. These packings were earlier used in the construction of the model of open-cell foam piece (Krishnan et al., 2008).
The centers of spheres are placed into the nodes of three-dimensional lattice. The lattice for the bcc model is constructed in such a way that every sphere intersects with 8 or 14 spheres depending on the packing density. The same spatial lattice is applied when packing the space with the other widely used elementary cell, the Kelvin cell, or tetrakaidecahedron (Kumar and Topin, 2014).
The geometry construction for the bcc model is done in ANSYS® DesignModeler®, and the whole process consists of several steps:
– creating fifteen equivalent spheres with radius *r*, nine at the nodes of the unit cell of the bcc lattice, and six at the centers of neighbourgh unit cells
– creating the cube with the size of the bcc lattice unit cell *a*
– cutting out the spheres from the cube; the foam strut structure is being formed
– applying cutting again to subtract the struts from the original cube; this way one obtains the repetitive foam unit cell (Figure 1)

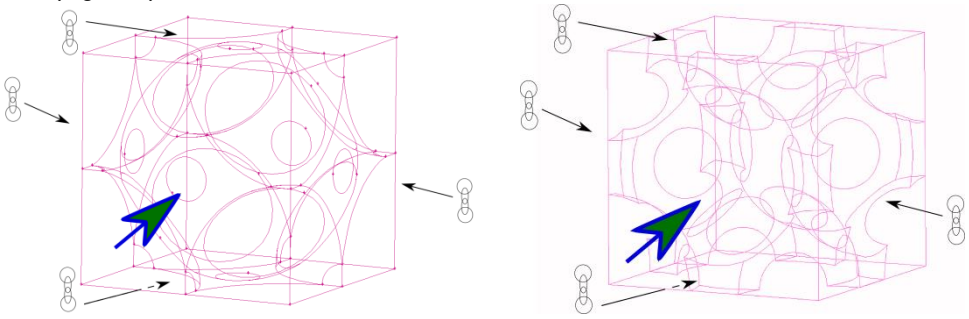

Figure 1: The bcc (left) and the fcc (right) repetitive foam unit cells. Faces with periodic boundary conditions are marked with the chain (⛓) sign. Flow direction is shown with the big arrow.

– the foam unit cell is translationally copied in the flow direction which is choosen as perpendicular to one of the unit cell faces.
The repetitive unit cell is not copied in two other directions that are perpendicular two unit cell faces due to the usage of geometry periodicity in those directions (Figure 1).
The fcc model is constructed applying the same procedure as for the construction of the bcc model, the only difference being the initial arrangement of spheres. For the fcc model each sphere has 12 neighbours independently of packing density for the whole range of *r/a* value that is allowed to preserve both permeability to the flow and struts connectivity.
The bcc geometry can represent the open-cell foam structure with a broad range of porosity (macroporosity, ε_M) values. The dependence of the porosity on the unit cell size *a* and sphere radius *r* is:

$$\varepsilon_M = \left(4\pi\sqrt{3}r^2a - \pi\sqrt{3}a^3/4 - 8\pi r^3\right)/a^3 \text{ , } 0.6802 < \varepsilon_M <= 0.9395; \quad (1)$$

$$\varepsilon_M = \left((4\sqrt{3}+6)\pi r^2 a - (2+\sqrt{3})\pi a^3/4 - 16\pi r^3\right)/a^3 \text{ , } 0.9395 < \varepsilon_M = 0.9945. \quad (2)$$

For the low porosity range, each cell is connected with eight neighbour cells, and for the high porosity range, each cell can exchange the fluid with 14 neighbours. As discussed by Gibson and Ashby (1997), each foam cell usually has 12-14 neighbours, and the models used are consistent with this guideline. The bcc model with eight faces could represent the open-cell foam with the moderate amount of closed cells.

2.2 Mesh

The unstructured tetrahedral finite volume mesh is prepared in ANSYS® Meshing®. The mesh construction is done for different values of total number of elements to make mesh independency check. The results of mesh independency study are presented in the following Results and Discussion section. The final meshes for the bcc and fcc structure (4 unit cells) contain 0.5-1.2 million cells depending on the modeled porosity.

The boundary layer is resolved with the use of inflation, i.e., an ordered mesh layers constiting of prisms are included into the near-wall region. Boundary layer compression is allowed to prevent boundary layer collision.

2.3 Mathematical model

The mathematical model used is based on Reynolds-Averaged Navier Stokes equations (RANS). These equations for the steady state flow of Newtonian fluid can be written as follows (the Einstein notation is implied and the averaging overbar is dropped) (ANSYS Inc., 2011):

$$\frac{\partial \rho u_i}{\partial x_i} = 0 \quad (4)$$

$$\frac{\partial \rho u_i u_j}{\partial x_j} = -\frac{\partial p}{\partial x_i} + \frac{\partial}{\partial x_j}\left[\mu\left(\frac{\partial u_i}{\partial x_j} + \frac{\partial u_j}{\partial x_i} - \frac{2}{3}\delta_{ij}\frac{\partial u_l}{\partial x_l}\right)\right] + \frac{\partial(-\rho\overline{u'_i u'_j})}{\partial x_j} \quad (5)$$

The flow in the open-cell foam is transitional or turbulent when pore diameter based Reynolds number $Re_p = ud_p\rho/\mu$ is higher than unity (Della Torre et al., 2014). So, the turbulent structures are needed to be resolved or modelled.

The choice of RANS-based turbulence modelling is dictated by the mesh size used, as it requires the lowest resources compared to other approaches (Large Eddy Simulation, or, Direct Numerical Simulation).

Realizable k-ε turbulence model was used to make the RANS equations system closed (ANSYS Inc., 2011).

The mesh used guarantees that the value of dimensionless distance to the wall, Y^+, is below 10. Due to Y^+ values range the turbulence model is used in conjuction with the Enhanced Wall Treatment approach (Ansys Inc., 2011). The curvature correction is also applied.

For the whole simulation the following parameters are used:

– cell diameter, as a diameter of spheres used for the model construction, d_{cell} = 2.11 mm;

– temperature – 298.15 K;

– pressure at outlet – 101,325 Pa;

– material properties: fluid – air (N_2 78 vol. %, O_2 21 vol. %, Ar 0.97 vol. %, CO_2 0.03 vol. %.), dynamic viscosity 1.785×10^{-5} Pa s, density 1.225 kg/m^3, solid wall – alumina.

Boundary conditions for k-ε turbulence model are:

– initial turbulence intensity at inlet – 5 %;

– hydraulic diameter at inlet – equal to the cell diameter.

Three porosity values are studied: ε_M = 0.85, 0.9, 0.95. The periodic boundary conditions are applied on two unit cube faces that are perpendicular to the flow direction (Figure 1).

The mathematical model is solved with the finite-volume code ANSYS® FLUENT®. The second order scheme is used for the spatial discretization. The evaluation of gradients is done according to the least squares cell-based method. The pressure-based segregated algorithm is choosen to solve the governing equations; the pressure correction is done using the SIMPLE method (Patankar, 1980).

3. Results and discussion

The results of the mesh independence check (not shown) points out that the mesh with 14 layers could provide pressure drop prediction error of less than 5 % in comparison with the highest refined mesh studied, and it is used for all subsequent calculations.

It is important to study how the pressure drop varies with the porosity at the same value of velocity (Figure 2). The velocity used is a superficial velocity, volumetric flow rate per unit-cell cross section a^2. The lower pressure drop values are obtained with the higher porosity values, the simulation results does not contradict the experimental data (Tishchenko et al., 2005). This proves the physical consistency of models.

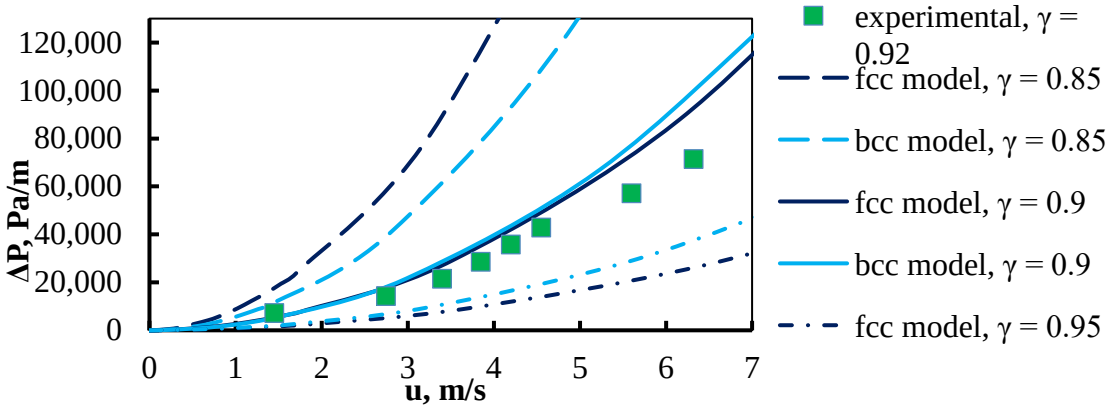

Figure 2: Pressure drop as a function of superficial velocity at different values of porosity. Dark lines – the fcc model, light lines – the bcc model. Line type: dashed, ε_M = 0.85; solid, ε_M = 0.90; dash-dotted, ε_M = 0.95

The bcc model provides a larger pressure drop values for the high foam porosity (95 %). The two models give similar predictions for 90 % porosity. With the subsequent porosity decrease to 85 % the fcc model starts to give a higher pressure drop. Therefore, the fcc model has a higher sensitivity of pressure drop on porosity.
The velocity distribution plotted at the same values of porosity and superficial velocity for two models (Figure 3) is slightly wider for the fcc model. It can be seen that the maximal velocity is reached near the sharp corners of struts. The bcc model has two types of struts, one having the long side perpendicular to the flow (let us call them wide), and the other having the long side parallel to the flow (narrow). The largest recirculation zone is located near the wide struts of the bcc model. The fcc model also predicts larger recirculation zone near the strut edges that are aligned with the flow, because the struts are more concave. The concave struts are formed when manufacturing open-cell foam with high porosity (> 0.95) values (Inayat et al., 2015). A boundary layer is very thin near the sharp strut corners and this would provides a fast mass tranfer to the zone nearby the strut corners.

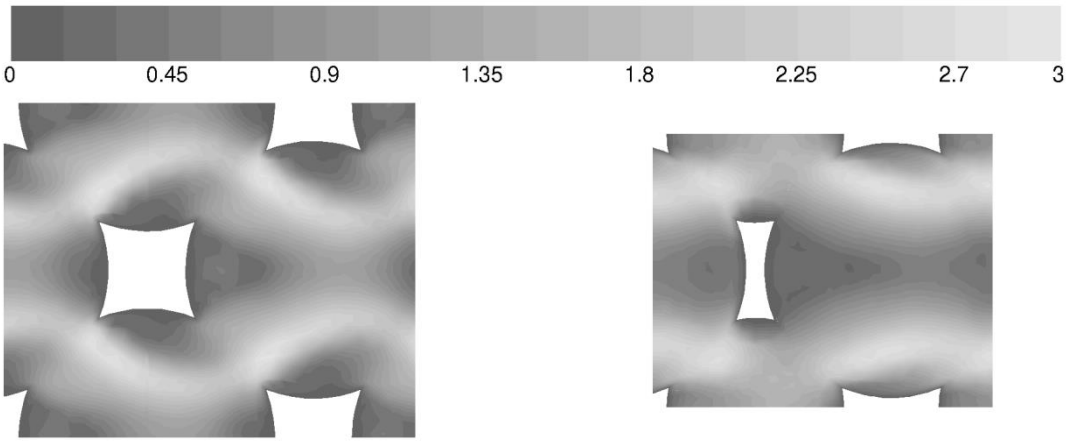

Figure 3: Contours of velocity magnitude at superficial velocity equal to 0.88 m/s and ε_M = 0.9. Left – the fcc model, right – the bcc model. Maximal internal averaged velocity u_{max} = 3.00 m/s (fcc) and 2.92 m/s (bcc).

Comparing values of mass-weighted flow uniformity index ψ (ANSYS Inc., 2011) at different values of inlet u_{inlet} velocity (Table 1) one may note that the most uniform flow is reached at the simultaneous highest porosity and velocity values (turbulent flow). The lowest values ψ values are observed at intermediate velocity of 1 m/s. This corresponds to the transitional regime (see below). Also, the data in Table 1 confirm flow uniformity increase with the increase of porosity.

Table 1: Mass-weighted flow uniformity index, ψ

bcc model				fcc model			
ε_M	u_{inlet}, m/s	mean ψ throughout the model	mean ψ at outlet	ε_M	u_{inlet}, m/s	mean ψ throughout the model	mean ψ at outlet
0.85	0.05	0.8584	0.8683	0.85	0.05	0.8186	0.8337
0.85	1.0	0.8242	0.8606	0.85	1.0	0.7928	0.7946
0.85	7.0	0.8578	0.8747	0.85	7.0	0.8214	0.8102
0.90	0.05	0.8783	0.8778	0.85	0.05	0.8599	0.8487
0.90	1.0	0.8229	0.8553	0.85	1.0	0.8320	0.8557
0.90	7.0	0.8634	0.9021	0.85	7.0	0.8636	0.8631
0.95	0.05	0.8718	0.8873	0.85	0.05	0.8914	0.8723
0.95	1.0	0.8397	0.8677	0.85	1.0	0.8613	0.8757
0.95	7.0	0.8653	0.9195	0.85	7.0	0.8849	0.9100

Turbulent intensity is a ratio of mean fluctuation velocity to the mean averaged velocity:

$$I = u' \Big/ \left|\bar{u}\right| = \sqrt{2k/3} \Big/ \left|\bar{u}\right| \tag{8}$$

In contrast to the flow uniformity index, the turbulent intensity is a measure of a local deviation from the averaged velocity, not in the averaged velocity throughout the geometry domain. It indicates the presence of turbulent chaotic eddies and pulsations. Note, the current definition uses the local averaged velocity magnitude in the denominator and differs from one based on the reference velocity (ANSYS Inc., 2011).

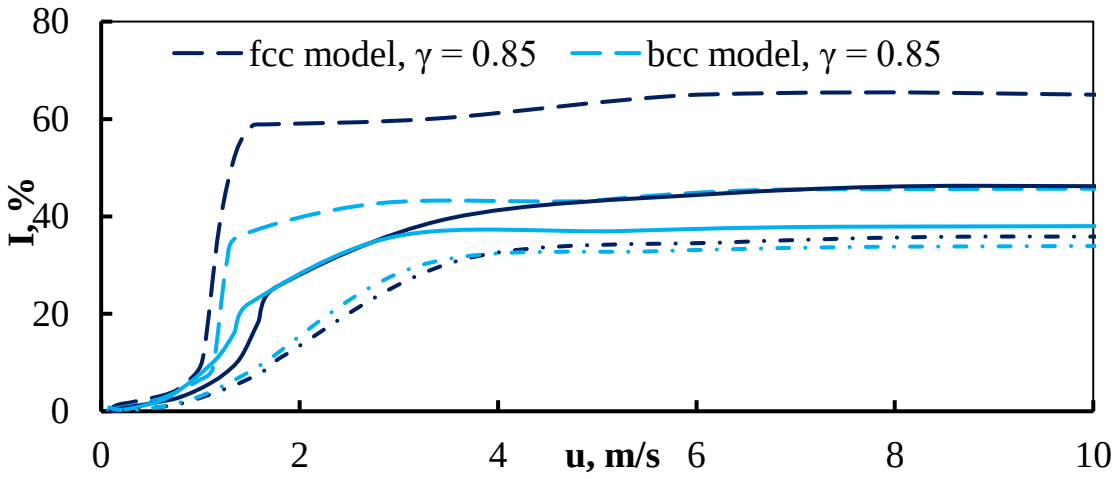

Figure 4: Turbulence intensity for the different values of porosity. The notation used is as for the Figure 3

The high turbulence intensity values (Figure 4) confirm the early transition to turbulence in open-cell foams, which was observed earlier by different authors (Mitrichev et al., 2012) and (Della Torre et al., 2014). It finishes faster with the porosity decrease.

It is interesting to compare the bcc and the fcc structure as the possible foam structures for process intensification. The first intensifiction goal is the most effective mixing realizable with the higher turbulence intensity. The second goal is to achieve the lower pressure drop. The highest turbulence intensity is observed on the fcc model with the lowest porosity studied. The fcc structure with 85 % porosity would turbulize the flow in a more efficient way than the bcc structure in a case of process operating under mass-transfer limiting conditions. However, this structure have shown the largest pressure drop.

If the pressure drop value would be inappropriate for the specific application and would enforce the usage of 90% porosity foam, the bcc structure should be used with the low velocity values and the fcc structure – with moderate and high velocity values (Figure 4). At 95 % porosity level the turbulence intensity is slightly higher for the bcc structure than for the fcc structure at low velocities. However, at moderate and high velocity values (as well as with respect to the pressure drop) the fcc structure outperforms the bcc structure.

The turbulence intensity values for the case of 90 % porosity are in agreement with those obtained with the use of RNG k-ε model (Mitrichev et al., 2012).

4. Conclusions

A comparison of two geometrical models of open-cell foam, the bcc and the fcc model, shows that the fcc model predicts more severe changes in the pressure drop with the decrease of porosity. High values of mass-weighted flow uniformity index (0.8-0.9) are observed, the uniformity being increased with the increase of porosity. It indicates the good mixing of the flow and a low thickness of boundary layer. The boundary layer is especially thin at the sharp strut edges.

The calculated high values of turbulence intensity indicate the early transition to turbulence and high turbulence level. The transition to the turbulent regime occures faster for the low porosity foams. The most intensive fluctuations occure in the fcc structure with the lowest studied porosity (85 %).

The results could be applied for the intensification of processes operating in a mass-transfer limiting mode, such as catalytic wall surface reactions. The optimal foam structure would be then a compromise between turbulence intensity and total pressure drop.

Acknowledgments

The work was supported by the Russian Foundation of Basic Research (RFBR), project 14-07-00960.

References

ANSYS Inc., 2011, ANSYS FLUENT Theory Guide, Release 14.0, Canonsburg, PA, USA, 794 p.

Bach C., Dimopoulos Eggenschwiler P., 2011, Ceramic Foam Catalyst Substrates for Diesel Oxidation Catalysts: Pollutant Conversion and Operational Issues, SAE Technical Paper 2011-24-0179, DOI: 10.4271/2011-24-0179

Della Torre A., Montenegro G., Tabor G.R., Wears M.L., 2014, CFD characterization of flow regimes inside open cell foam substrates, Int. J. Heat Fluid Flow 50, 72-82, DOI: 10.1016/j.ijheatfluidflow.2014.05.005

Dukhan N., Suleiman A.S., 2014, Simulation of entry-region flow in open-cell metal foam and experimental validation, Transp. Porous Media 101, 2, 229-246, DOI: 10.1007/s11242-013-0241-z

Gibson L.J., Ashby M.F., 1997. Cellular Solids. Cambridge University Press, Cambridge, UK.

Hutter C., Zenklusen A., Kuhn S., von Rohr P.R., 2011, Large eddy simulation of flow through a streamwise-periodic structure. Chem. Eng. Sci. 66, 3, 519-529, DOI: 10.1016/j.ces.2010.11.015

Inayat A., Klumpp M., Lämmermann M., Freund H., Schwieger, W., 2016, Development of a new pressure drop correlation for open-cell foams based completely on theoretical grounds: Taking into account strut shape and geometric tortuosity, Chem. Eng. J. 287, 704-719, DOI: 10.1016/j.cej.2015.11.050

Krishnan S., Murthy J. Y., Garimella S. V., 2006, Direct simulation of transport in open-cell metal foam, ASME J. Heat Transfer 128, 793–799, DOI: 10.1115/1.2227038

Krishnan S., Garimella S.V., Murthy J.Y., 2008, Simulation of thermal transport in open-cell metal foams: effect of periodic unit-cell structure, ASME J. Heat Transfer 130, 2, 024503. DOI: 10.1115/1.2789718

Kumar P., Topin F., 2014, Investigation of fluid flow properties in open cell foams: Darcy and weak inertia regimes, Chem. Eng. Sci. 116, 793-805, DOI: 10.1016/j.ces.2014.06.009

Lucci F., Della Torre A., Montenegro G., Eggenschwiler P. D., 2015, On the catalytic performance of open cell structures versus honeycombs, Chem. Eng. J. 264, 514-521, DOI: 10.1016/j.cej.2014.11.080

Mitrichev I.I., Koltsova E.M., Zhensa A.V., 2012, Computer simulation of gasodynamic conditions in channels of open-cell foam, Fundamental research 11, 2, 440-446 (in Russian)

Palma V., Ricca A., Ciambelli P., 2012, Monolith and foam catalysts performances in ATR of liquid and gaseous fuels, Chem. Eng. J. 207, 577-586, DOI: 10.1016/j.cej.2012.07.018

Palma V., Ruocco C., Ricca A., 2015, Bimetallic Pt and Ni Based Foam Catalysts for Low Temperature Ethanol Steam Reforming Intensification, Chem. Eng. Trans., 43, 559-564, DOI: 10.3303/CET1543094

Patankar S.V., Numerical Heat Transfer and Fluid Flow, Hemisphere, Washington D.C., USA, 1980. 197 p.

Pozzobom I.E.F., De Moraes G.G., Balzer R., Probst L.F.D., Trichês E.S., Novaes De Oliveira A.P., 2015, Glass-Ceramics Foam for Hydrogen Production, Chem. Eng. Trans. 43, 1783-1788, DOI: 10.3303/CET1543299

Volkov K.N., Emelyanov V.N., 2008, Large Eddy Simulation in Calculations of Turbulent Flows, Fizmatlit, Moscow, Russia, 368 p (in Russian)